Specific heat of multifractal energy spectra

L. R. da Silva,[1,*] R. O. Vallejos,[2,†] C. Tsallis,[3,4,‡] R. S. Mendes,[5,§] and S. Roux[6,‖]

[1]*Departamento de Fisica Teorica e Experimental, Universidade Federal do Rio Grande do Norte, 59072-970 Natal, RN, Brazil*

[2]*Instituto de Fisica, Universidade Estadual do Rio de Janeiro, Rua São Fransisco Xavier 524, 20559-900 Rio de Janeiro, RJ, Brazil*

[3]*Massachusetts Institute of Technology, 77 Massachusetts Avenue - R. 3-164 Cambridge, MA 02139*

[4]*Centro Brasileiro de Pesquisas Fisicas, Rua Xavier Sigaud 150, 22290-180 Rio de Janeiro, RJ, Brazil*

[5]*Departamento de Fisica, Universidade Estadual de Maringá, 87020-900 Maringa, PR, Brazil*

[6]*Laboratoire ''Surface du Verre et Interfaces,'' Unité Mixte de Recherche CNRS/Saint-Gobain, 39 Quai Lucien Lefranc, 93303 Aubervilliers Cedex, France*

(Received 28 September 2000; published 12 June 2001)

Motivated by the self-similar character of energy spectra demonstrated for quasicrystals, we investigate the case of multifractal energy spectra, and compute the specific heat associated with simple archetypal forms of multifractal sets as generated by iterated maps. We considered the logistic map and the circle map at their threshold to chaos. Both examples show nontrivial structures associated with the scaling properties of their respective chaotic attractors. The specific heat displays generically log-periodic oscillations around a value that characterizes a single exponent, the ''fractal dimension,'' of the distribution of energy levels close to the minimum value set to 0. It is shown that when the fractal dimension and the frequency of log oscillations of the density of states are large, the amplitude of the resulting log oscillation in the specific heat becomes much smaller than the log-periodic oscillation measured on the density of states.

DOI: 10.1103/PhysRevE.64.011104 PACS number(s): 05.20.−y, 61.43.Hv, 65.40.−b, 61.44.Br

I. INTRODUCTION

In recent years there has been an increasing interest in quasicrystals. These peculiar structures have been studied extensively both experimentally [1] and theoretically [2]. Several reviews on the subject are available [3]. One fascinating observation concerns the scaling property of some physical properties observed on those systems. In particular, excitations or quasiparticle states exhibit self-similar spectra [4]. In order to better understand the thermodynamics of such objects, model cases have been studied [5–8]. In particular in Refs. [6–8] the specific heat $C(T)$ has been computed for fractally distributed energy spectra. The present contribution follows similar lines, through the investigation of more general energy spectra, namely, multifractal ones [9]. For this purpose, we consider a few strange attractors of iterated maps at the onset of chaos that have been studied in detail in the past and map the attractor on the energy levels ϵ_n, $n=1,2,\ldots$.

The main conclusion of the initial studies on the specific heat is that it saturates for low temperature at a value that corresponds to the fractal dimension of the fractal support. Moreover, this saturation is ''decorated'' by oscillations in $\ln(T)$. Thus the period of these oscillations decreases as T vanishes. The origin of these oscillations was identified to be due to an intrinsically discrete self-similarity of the deterministic fractal considered as in a number of other examples studied in Ref. [10]. The same oscillations could be directly identified as the longest wavelength oscillations on the integrated density of states when it is expressed in terms of the logarithm of the energy. We will see that most of the conclusions reached on the Cantor sets are still applicable to this more complicated class of energy spectra. Let us also note that such oscillating specific heat has been obtained in an aperiodic Ising model [11]. Moreover, recently Curado and Rego-Monteiro [12] derived similar multifractal spectra such as the ones we will study below directly from a Hamiltonian, and not as postulated spectrum as we do here.

In the present study, after defining our identification of the energy spectrum, we present the result of direct numerical simulations, concerning the cumulative density of states and the specific heat. We give a closed form expression for the amplitude of the log oscillations that are expected in the specific heat, and we show that when the frequency is high (typically larger than unity in the natural scale of the problem) the amplitude of the oscillations is rapidly decaying due to intrinsic filtering that can be related to the form of the Boltzmann weight. Finally, we discuss the relevance of multifractality in the present problem.

II. ENERGY SPECTRA

We considered two iterated maps at the onset of chaos: the logistic and the circle maps. They follow a similar structure, namely, one computes the values of the sequence

$$x_{n+1}=\phi(x_n;A) \tag{1}$$

for a control parameter A. For low enough values of A, the set of points x_n ends on a periodic orbit. At a critical value of $A=A_c$, the attractor of x_n becomes a fractal object, and the

*Email address: luciano@dfte.ufrn.br
†Email address: vallejos@cbpf.br
‡Email address: tsallis@cbpf.br
§Email address: rsmendes@dfi.uem.br
‖Email address: stephane.roux@saint-gobain.com

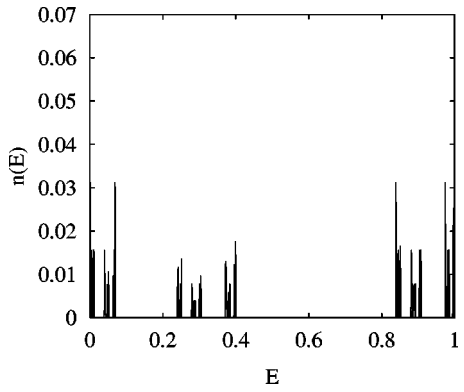

FIG. 1. Plot of the density of states $n(E)$ for the logistic map at the onset of chaos.

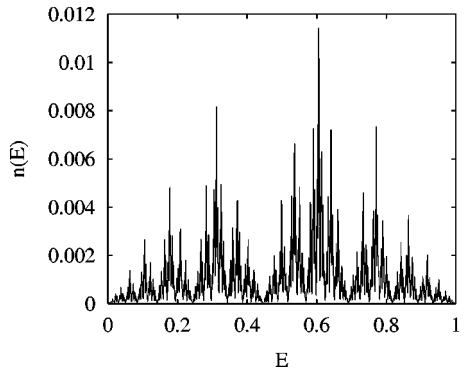

FIG. 2. Plot of the density of states $n(E)$ for the circle map at the onset of chaos.

distribution of x on this set becomes multifractal. Past A_c the iteration can be chaotic. These features are quite general and can be encountered in many examples, and they illustrate one of the possible scenarios of the transition to chaos. We specialize our discussion in the following on two such maps.

The iterated values of x_n are then identified with energy levels E_n after a translation and dilation so that E_n fit into the interval $[0:1]$

$$E_n \equiv \frac{x_n - \min\{x_i\}}{\max\{x_i\} - \min\{x_i\}}. \tag{2}$$

In the cases of interest for us in the following, the computation of the ground state energy, $\min\{x_i\}$, is straightforward. The latter plays a central role in the analysis, since by changing the temperature, we will analyze the scale invariant nature of the energy spectrum with respect to a dilation from the ground state value.

Let us now define the maps used hereafter.

A. Logistic map

The most classical example is the logistic map [13] defined as

$$\phi_{log}(x) = 1 - Ax^2. \tag{3}$$

The critical value of A is $A_c = 1.401\,155\,198\ldots$. The density of states is shown in Fig. 1.

B. Circle map

The second case is the circle map [13], defined by the following iteration function

$$\phi_{cir}(x) = A + \left(x - \frac{\sin(2\pi x)}{2\pi} \right) \pmod 1 \tag{4}$$

where the critical value of A is $A_c = 0.606\,661\,063\,469\ldots$. The density of states can be seen in Fig. 2. We observe that the support of the energy level is much denser than in the previous case, in agreement with the observation that the fractal dimension of the support is unity.

For reasons discussed latter, we also consider as a variant in this case the energy level E_n as given by a power law of the iterated x_n,

$$E_n = x_n^{\beta}, \tag{5}$$

where β is an arbitrary parameter. (Note that in this last case, the minimum and maximum values of x are 0 and 1, respectively.)

III. NUMERICAL RESULTS

Once a large number of energy levels have been generated (typically 10^6), the partition function $Z(T)$ is computed as a function of temperature, using the standard Boltzmann measure

$$Z(T) = \sum_n e^{-E_n/kT}, \tag{6}$$

where the Boltzmann constant k is set to unity, thereby defining our temperature scale. We also computed the integrated density of states

$$N(E) = \sum_n H(E_n - E), \tag{7}$$

where H is the Heaviside function (equal to 1 for positive arguments and 0 for negative ones). Finally, we computed the specific heat as

$$C(T) = \left(\frac{1}{T^2} \right) \left[\frac{\sum_n E_n^2 e^{-E_n/kT}}{Z(T)} - \left(\frac{\sum_n E_n e^{-E_n/kT}}{Z(T)} \right)^2 \right] \tag{8}$$

Figure 3 shows the log-log plot of the cumulative density of states of the energy levels obtained from the logistic map. The dotted line drawn in the same figure indicates that the large scale trend of the density of states is to grow as a power law of the energy,

$$N(E) \propto E^D, \tag{9}$$

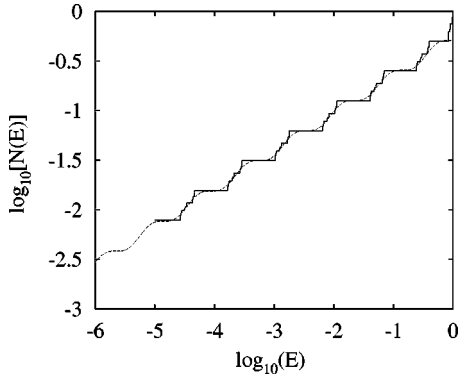

FIG. 3. Log-log plot of the integrated density of states $N(E)$ for the logistic map at the onset of chaos. The dotted curve shows a best fit to the data using a single log oscillation.

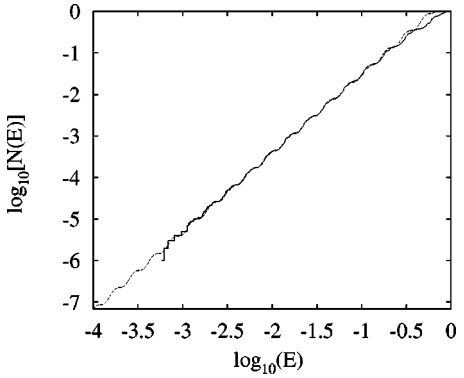

FIG. 4. Log-log plot of the integrated density of states $N(E)$ for the circle map at the onset of chaos. The dotted curve shows a best fit to the data using a single log oscillation.

with an exponent that can be compared with the fractal dimension for the Cantor sets that were studied previously. However, on top of the power-law increase, we see a characteristic periodic pattern that rather reflects a discrete self-similarity, which is a characteristic of the iterated map in the same way as other characteristic exponents. Following the spirit of the analysis presented in Ref. [7], we can Fourier decompose $\ln[N(E)E^{-D}]$ as a function of $\ln(E)$ and obtain

$$\ln[N(E)] = D\ln(E) + \sum_{n=-\infty}^{\infty} A_n \exp\{2i\pi n\omega \ln(E)\}, \tag{10}$$

where ω is the fundamental frequency of the (logarithmic) density of states, and A_n is the complex Fourier amplitude, with $A_{-n} = \overline{A_n}$. Retaining only the lowest frequency part of the decomposition, we arrive at the following approximation for the density of states

$$N(E) \approx AE^D + BE^{D+2i\pi\omega} + \overline{B}E^{D-2i\pi\omega}, \tag{11}$$

where $A = e^{A_0}$ is a real and $B = e^{A_0}A_1$ is a complex amplitude. The above formula relies on the fact that the oscillating amplitude is small, $|B|/A \ll 1$, so that the higher harmonics can be neglected. We note that the fact that N is a nondecreasing function imposes $|B|/A < 1$ for any energy spectrum. Thus our approximation is believed to be of wide applicability. Moreover, as $|B|/A$ increases, the quality of the approximation will become worse, but no dramatic change of behavior will take place. We thus see that the log oscillations are due to the presence of two complex conjugated ''fractal dimensions'' $D \pm 2i\pi\omega$ and a real one D having an identical real part. We have plotted on Fig. 3 as a dotted line such an approximation. We see that it captures the main trends of the data. For the logistic map, we estimate $D \approx 0.38$ and $\omega \approx 0.54$. The amplitude of the oscillation is observed to be small, $A \approx 0.89$ and $|B|/A \approx 0.02$.

A similar behavior can be observed on the circle map, as shown in Fig. 4. The corresponding parameters are estimated to be $D = 1.89$, $\omega \approx 2.0$, $A \approx 1.18$ and $|B|/A = 0.026$. The fact that the ''fractal dimension'' D is larger than one (i.e., the space dimension) is not to be considered as an offending value, it simply means that the number of energy levels grows faster than linearly with the energy level. It does not refer to a property of the *support* of those energies that obviously requires a fractal dimension smaller than or equal to unity.

The specific heat has been computed from Eq. (8), using 10^6 iterations. Figure 5 shows the obtained results, in a semilog scale. We do observe that for low temperatures, $C(T)$ oscillates around a mean value that precisely corresponds to the fractal dimension determined previously, as in the standard case of the Cantor sets, which were studied in the past [6,7]. We reproduce here the basic argument leading to this result.

From the approximate form of the integrated density of states Eq. (11), we can compute different moments of the energy, using the Boltzmann measure associated with a temperature T, or their natural rescaling with the temperature z_n defined as

$$z_n \equiv \frac{\langle E^n \rangle_B}{T^n} = \int N(E)[(E/T)^n - n(E/T)^{n-1}]e^{-E/T}dE/T. \tag{12}$$

From the latter moments, the specific heat is simply written

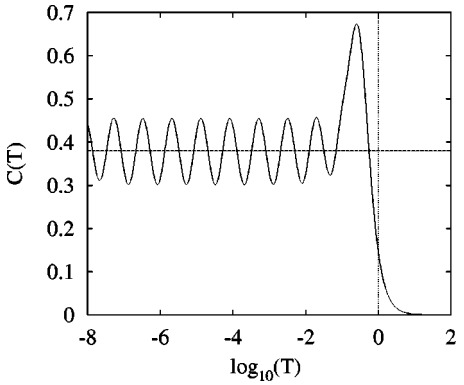

FIG. 5. Semilog plot of the specific heat computed from the logistic map energy spectrum. The dotted line corresponds to a value equal to D as determined from the integrated density of states.

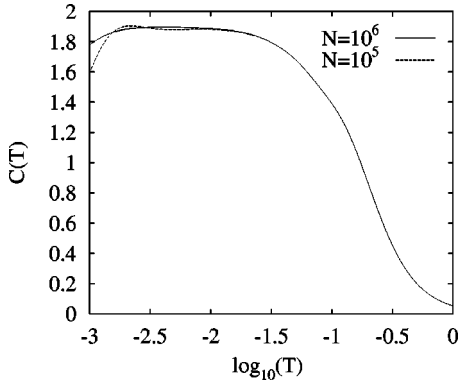

FIG. 6. Semilog plot of the specific heat computed from the circle map energy spectrum. The plain curve corresponds to 10^6 points while the dotted one is computed from 10^5. We see that a plateau develops at the value of the fractal dimension $D \approx 1.9$, but no oscillations are visible.

$$C(T)=\left(\frac{z_2}{z_0}\right)-\left(\frac{z_1}{z_0}\right)^2. \tag{13}$$

Using a power-law form for $N(T)$, i.e. neglecting B in Eq. (11), we obtain

$$z_n=AT^D\int_0^\infty x^D[x^n-nx^{n-1}]e^{-x}dx=AT^D(D+1)\Gamma(n+D), \tag{14}$$

where $\Gamma(\ldots)$ is the Euler function of second kind. From the latter expression, we deduce $C(T)=D(D+1)-D^2=D$. Incorporating the oscillating part, we have

$$\begin{aligned} z_n=AT^D[&(D+1)\Gamma(n+D)+(B/A)(D+1+2i\pi\omega)\\ &\times\Gamma(D+n+2i\pi\omega)T^{2i\pi\omega}+(\overline{B}/A)(D+1-2i\pi\omega)\\ &\times\Gamma(D+n-2i\pi\omega)T^{-2i\pi\omega}]. \end{aligned} \tag{15}$$

Considering that $|B|/A$ is a small parameter (what has been shown to be justified), we may expand the above formula and obtain

$$\begin{aligned} C(T)=D&+\frac{B}{A}\frac{2i\pi\omega D(1+2i\pi\omega)}{D+2i\pi\omega}\frac{\Gamma(D+2i\pi\omega+2)}{\Gamma(D+2)}T^{2i\pi\omega}\\ &-\frac{\overline{B}}{A}\frac{2i\pi\omega D(1-2i\pi\omega)}{D-2i\pi\omega}\frac{\Gamma(D-2i\pi\omega+2)}{\Gamma(D+2)}T^{-2i\pi\omega}. \end{aligned} \tag{16}$$

From this formula, we see that the specific heat has a mean constant part equal to the fractal dimension D and on top of it there is an oscillatory component at frequency ω whose amplitude is directly related to the amplitude of the oscillation in the density of states, with a prefactor that is unique function of D and ω. This result is a simple extension of the computation presented in Ref. [7].

We performed the computation of $C(T)$ for the circle map case. The result is presented in Fig. 6. We do observe as previously, that the specific heat tends to a constant value for low temperatures, and that this value is equal to the previously determined fractal dimension obtained from the density of states (see Fig. 4) but no oscillations can be detected.

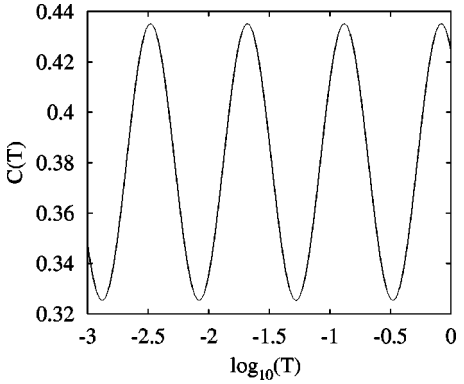

FIG. 7. Direct evaluation of the specific heat from the fitted density of states for the logistic map case. The result compares nicely to the direct calculation shown in Fig. 5.

The absence of oscillation is a puzzling fact, and in order to elucidate this question, we computed directly the specific heat not for the obtained energy levels, but from the fit to the density of states [Eq. (11)], which could be extrapolated down to very low values of the energy. The same procedure was applied to the logistic map. Figure 7 shows the result obtained for the latter case. We observe an excellent agreement with the direct integration, for the oscillating part. The large bump that is present in the direct computation (see Fig. 5) comes from the end of the spectrum and obviously breaks the scale invariance symmetry. Our analytical approximation does not reproduce this accident since the harmonic fit is extended to infinity.

In contrast, the similar computation performed for the circle map and whose results are shown in Fig. 8, we do recover the expected oscillations around the D value, however, we observe in this case that the amplitude of oscillations is dramatically smaller than in the logistic map case, 3.5×10^{-5}. This enlightens the reason why we did not observe the oscillations in the direct calculation.

One way of understanding the very abrupt decay of the amplitude of the oscillatory component is to note that the

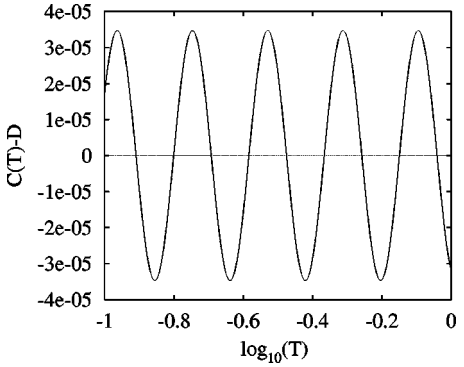

FIG. 8. Direct evaluation of the specific heat from the fitted density of states for the circle map case. We have substracted the mean value for clarity. Note that the amplitude of oscillation is of the order of 3.5×10^{-5}.

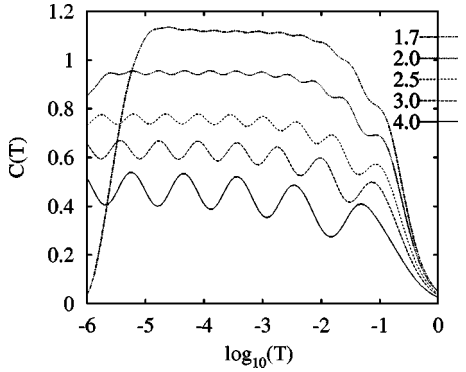

FIG. 9. Semilog plot of the specific heat of the generalization of the circle map, obtained by raising the energy level to a power β. The value of β is indicated in the caption. We note that for large β, the oscillatory behavior is well pronounced, around a value D/β and with a frequency ω/β. However, as β decreases, the amplitude of the oscillation is strongly damped, and the domain of scaling is reduced as T should be divided by β.

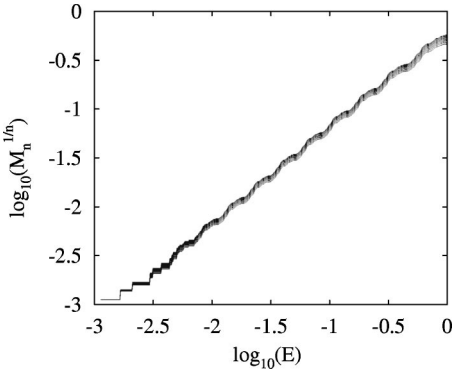

FIG. 10. Log-log plot of the moments $M_n^{1/n}$ of the energy levels computed from the origin up to level E. The moment order n ranges from 1/4 (top) to 9/4 (bottom) by steps of 1/4. The fact that all curves are parallel signals that the spectrum is not multifractal in the vicinity of the origin. This is to be contrasted with the global behavior that is known to be multifractal. Note that the log oscillations are quite visible.

partition function when expressed as a function of $\theta \equiv \ln(T)$ can be written as the convolution of the log density of states $n(\ln(E)) \equiv En(E)$, by the function $B(\theta)$ where B is

$$B(\theta) = \exp[-\exp(-\theta)]. \tag{17}$$

The first derivative is thus a convolution of the log density of density of states by $B'(\theta) = \exp[-\exp(-\theta)]\exp(-\theta)$. Thus we see that the Boltzmann weight term introduces a smoothening at the scale of the width of B', of order unity. This convolution will essentially preserve oscillations whose wavelength is larger than the width of B', whereas shorter oscillation will be very severly attenuated. We recall that the frequency of the logistic map is of order 0.54, whereas that of the circle map is of order 2.0. This accounts for the smooth behavior observed in the case of the circle map.

In order to prove that this high frequency is the main reason for the very active reduction of the oscillating amplitude of the specific heat, we considered the following construction. From the usual circle map, we compute the recursive iterates of ϕ, and we choose to attribute an energy level E_i to the value of the ith iterate raised to a power β as shown in Eq. (5). As β is increased from the value 1, we can easily understand the impact of this transformation on the shape of the integrated density of states curve. Only the $\ln(E)$ axis has to be scaled by β. Thereby the fractal dimension of the density of states is simply rescaled by β, $D = D/\beta$. Similarly, the frequency is decreased to ω/β. Thus, the amplitude of the oscillation should be large for large β, and it should decrease strongly as the frequency becomes much smaller than unity.

To test this prediction, we computed the specific heat of the modified density of states for the circle map, for various values of β. The results are shown in Fig. 9. We do observe as expected that for large β, the specific heat displays large oscillations, but the latter are reduced significantly for smaller values. We thus conclude that although we did not observe the oscillation for the circle map case ($\beta = 1$), they still exist, but have been damped so drastically that we cannot detect them within reasonable values of computed energy levels.

IV. MULTIFRACTALITY

Finally, up to now we left aside the question of multifractality, and its possible impact on the scaling of the specific heat. Multifractality has been introduced in order to describe a more general class of fractal object such that various moments of the density would display independent power-law behaviors. More precisely, if we compute the nth order moment of the energy distribution within a fixed ''distance'' ΔE, from any level E_i in the spectrum, and average over all possible position of E_i, we expect to measure

$$M_n(\Delta E) \propto \Delta E^{\tau(n)}. \tag{18}$$

The set of exponents $\tau(n)$ could equivalently be represented by its Legendre transform that is often called the multifractal spectrum $f(\alpha)$. A single fractal, in this language obeys a ''constant gap scaling,'' i.e., $\tau(n)$ is an affine function of n, $\tau(n) = -\alpha_0 n + f_0$, and its multifractal spectrum is reduced to a point (α_0, f_0). For the two iteration maps considered in this study, the corresponding multifractal spectra have been studied in details in the past [13]. Let us note that in general, these multifractal spectra are inhomogeneous in space.

For our application, the energy levels are not all equivalent. The fundamental level set to zero for our purpose is a reference point from which the first and second moments (with a Boltzmann weight) are taken into account in the specific heat. In order to check the influence of selecting one special point, we computed the scaling of various moments of the energy levels from the following definition

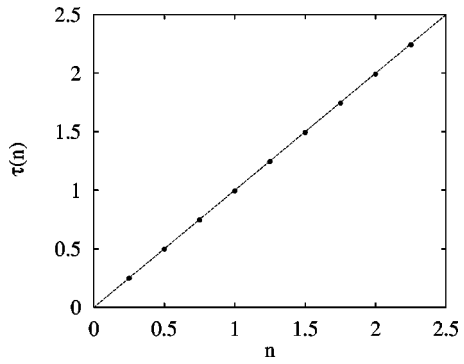

FIG. 11. The symbols show the exponents $\tau(n)$ of the scaling of the moments M_n with E, plotted versus the moment order n. The dotted line is $\tau=n$ that fits the data very well, thus showing that the scaling of the energy levels close to the origin is monofractal.

$$M_n(E)=\frac{\sum_{E'=0}^{E'=E} E'^n}{\sum_{E'=0}^{E'=E} 1}. \tag{19}$$

Note that we introduced a normalizing factor, (moment of order zero) which is precisely the integrated density of states. Hence, we have $M_0(E)=1$ for all energies and thus $\tau(0)=0$ In order to check for the multifractal distribution, we plotted the moments M_n raised to the power $1/n$ as a function of E, as shown in Fig. 10. Surprisingly enough we observe that all moments are essentially parallel to each other (at least in the range of n values considered, i.e., $0.25\leqslant n\leqslant 2.25$. A more direct evaluation of the scaling exponents $\tau(n)$ shown in Fig. 11 obtained by a linear regression through the data shows that

$$\tau(n)=n. \tag{20}$$

Therefore, we conclude that for moments considered with respect to the fundamental level, there is no sign of multifractality. This result, in apparent contradiction with the classical results published for this problem simply underlines the special role played by the lowest point. In the case of iterated maps, it appears that multifractality might be associated with a fractal dimension that may vary from point to point in the strange attractor. Another possible interpretation is that we consider here that the energy levels have no width. As the map at the onset of chaos is not periodic, the system cannot revisit twice the same level. Thus, we have at most one energy level at a given point. If no broadening of the energy levels to a finite interval is considered, all moments will essentially probe the fractal dimension of the support of the energy spectrum. As a natural consequence, all moments can simply be related to the self-similar structure of the attractor close to the origin, and thus only to the property captured in the cumulative density of states.

V. CONCLUSION

We have considered in this study the specific heat associated with two examples of multifractal energy level distribution obtained from iterated maps (logistic and circle). We also studied other maps such as the periodic map [13], and although we did not report the results in this article, we obtained results that were quite comparable to the logistic map. We have shown that the basic properties that were first enlightened in the Refs. [6,7] in the case of Cantor sets, were also shown to be valid. This concerns the low temperature behavior of the specific heat that oscillates around a value equal to the fractal dimension of the energy levels close to the fundamental. The amplitude of the oscillations was shown to decrease in a drastic fashion as the frequency of the log oscillation of the density of states becomes larger than unity. This may even prevent their practical observation, as is the case for the circle map. Finally, we have shown that the reason of the wide applicability of the Cantor set result is that, albeit the entire attractor is known to be multifratal, the distribution of points close to the fundamental level follows a monofractal ditribution, and thus the scaling of the density of states close to the fundamental level is sufficient to compute the specific heat.

ACKNOWLEDGMENTS

S.R. acknowledges the warm hospitality of the Federal University of Rio Grande do Norte where this work was completed. We also acknowledge useful discussions with M.L. Devaney, E.M.F. Curado, and M.A. Rego-Monteiro. This work was supported in part by CNPq, FAPERJ and PRONEX/FINEP (Brazilian Agencies).

[1] D. Shechtman, I. Blech, D. Gratias, and J. W. Cahn, Phys. Rev. Lett. **53**, 1951 (1984); D. Levine and P. J. Steinhardt, *ibid.* **53**, 2477 (1984); R. Merlin, K. Bajema, R. Clarke, F. Y. Juang, and P. K. Bhattacharya, *ibid.* **55**, 1768 (1985); J. Todd, R. Merlin, R. Clarke, K. M. Mohanty, and J. D. Axe, *ibid.* **57**, 1157 (1986); K. Bajema and R. Merlin, Phys. Rev. B **36**, 4555 (1987); R. Merlin and K. Bajema, J. Phys. (Paris), Colloq. **48**, C5-503 (1987); Z. Cheng, R. Savit, and R. Merlin, Phys. Rev. B **37**, 4375 (1988).

[2] J. M. Luck and D. Petritis, J. Stat. Phys. **42**, 289 (1986); M. Kohmoto, B. Sutherland, and K. Iguchi, Phys. Rev. Lett. **58**, 2436 (1987); M. Kohmoto, B. Sutherland, and C. Tang, Phys. Rev. B **35**, 1020 (1987); R. Riklund, M. Severin, and Y. Liu, Int. J. Mod. Phys. B **1**, 121 (1987); J. M. Luck, Phys. Rev. B **39**, 5834 (1989); C. Sire, Europhys. Lett. **10**, 483 (1989); J. Bellisard, A. Bovier, and J. M. Ghez, Commun. Math. Phys. **135**, 379 (1991); F. Axel and H. Terauchi, Phys. Rev. Lett. **66**, 2223 (1991); E. Maciá, F. Domínguez-Adame, and A. Sánchez, Phys. Rev. B **49**, 9503 (1994); A. Rüdinger and C. Sire, J. Phys. A **29**, 3537 (1996).

[3] P. A. Lee and T. V. Ramakrishnan, Rev. Mod. Phys. **57**, 287 (1985); J. B. Sokoloss, Phys. Rep. **126**, 189 (1985); P. J. Stein-

hardt and S. Ostlund, *The Physics of Quasicrystals* (World Scientific, Singapore, 1987); D. di Vicenzo and P. J. Steinhardt, *Quasicrystals: The State of the Art* (World Scientific, Singapore, 1991); C. Janor, *Quasicrystals: A Primer* (Oxford University Press, Oxford, 1993); M. Senechal *Quasicrystals and Geometry* (Cambridge University Press, Cambridge, 1995).

[4] G. Y. Oh and M. H. Lee, Phys. Rev. B **48**, 12 465 (1993); E. L. Albuquerque and M. G. Cottam, Phys. Rep. **233**, 67 (1993); P. M. C. de Oliveira, E. L. Albuquerque, and A. M. Mariz, Physica A **227**, 206 (1996); M. Quilichini and T. Janssen, Rev. Mod. Phys. **69**, 277 (1997).

[5] H. Saleur and D. Sornette, J. Phys. I **6**, 327 (1996); Y. Meurice, S. Niermann, and G. Ordaz, J. Stat. Phys. **87**, 237 (1997); A. Arneodo, E. Bacry, S. Jaffard, and J. F. Muzy, *ibid.* **87**, 179 (1997); D. Karevsky and L. Turban, J. Phys. A **29**, 3461 (1996).

[6] C. Tsallis, L. R. da Silva, R. S. Mendes, R. O. Vallejos, and A. M. Mariz, Phys. Rev. E **56**, R4922 (1997).

[7] R. O. Vallejos, R. S. Mendes, L. R. da Silva, and C. Tsallis, Phys. Rev. E **58**, 1346 (1998).

[8] R. O. Vallejos and C. Anteneodo, Phys. Rev. E **58**, 4134 (1998).

[9] B. B. Mandelbrot, J. Fluid Mech. **62**, 331 (1974); P. Grassberger, Phys. Lett. A **97**, 227 (1983); H. G. E. Hentschel and I. Procaccia, Physica D **8**, 435 (1983); P. Grassberger and I. Procaccia, Phys. Rev. A **28**, 2591 (1983); Phys. Rev. Lett. **50**, 364 (1983); R. Benzi, G. Paladin, G. Parisi, and A. Vulpiani, J. Phys. A **17**, 3521 (1984); M. J. Feigenbaum, J. Stat. Phys. **46**, 919 (1987); T. C. Halsey, M. H. Jensen, L. P. Kadanoff, I. Procaccia, and B. I. Shraiman, Phys. Rev. A **33**, 1141 (1986); C. Beck and F. Schlogl, *Thermodynamics of Chaotic Systems* (Cambridge University Press, Cambridge, 1993).

[10] D. Sornette, Phys. Rep. **297**, 239 (1998).

[11] R. F. S. Andrade, Phys. Rev. E **59**, 150 (1999); **61**, 7196 (2000).

[12] E. M. F. Curado and M. A. Rego-Monteiro, Phys. Rev. E **61**, 6255 (2000).

[13] R. L. Devaney, *An Introduction to Dynamical Systems* (Addison-Wesley, Reading, 1989).